Adsorption (2011) 17: 311–323
DOI 10.1007/s10450-010-9288-0

# New mixing rule for predicting multi-component gas adsorption

**M. Mofarahi · S.A. Hashemifard**

Received: 30 June 2008 / Accepted: 21 October 2010 / Published online: 3 November 2010


**Abstract** The present work describes a predictive model for ascertaining the multi-component gas adsorption equilibria. The model utilizes special form of covolume-dependent (CVD) mixing which is combined with the generalized form of 2-D EOS. Four well known 2-D EOSs; van der Waals, Soave-Redlich-Kwong, Peng-Robinson, Eyring along with the modified CVD mixing rule were used to predict the total adsorption of several binary and ternary systems. Based on the concept of the CVD mixing rule, it was inspired that CVD mixing rule could be a binding bridge between the molecular size and the molecular interaction. To show this, the ratio of the classical mixing rule *%AAD* to the CVD mixing rule *%AAD* were plotted versus the difference of the collision or the Leonard-Jones diameters of the gas molecules in the mixtures. It shows that there is a criterion between the CVD and the classical mixing rules in terms of molecular size difference. It seems that, $\Delta\sigma_{LJ} \approx 0.60$ Å is the criterion. The CVD mixing rule is approximately predominant in the region of $\Delta\sigma_{LJ} \geq 0.60$ Å, whilst, region of $\Delta\sigma_{LJ} \leq 0.60$ Å is nearly governed by the classical mixing rule. All predictions by the new mixing rule and the classical mixing rule were compared with the experimental data from the case studies. The new form of the mixing rule is in good agreement with the experimental data even for the non-ideal systems; hence provides a powerful framework to predict multi-component gas adsorption.

M. Mofarahi (✉) · S.A. Hashemifard
Chemical Engineering Department, Engineering Faculty, Persian Gulf University, Bushehr 7516913817, Iran
e-mail: mofarahi@pgu.ac.ir

S.A. Hashemifard
e-mail: Salhashemifard@yahoo.com

**Keywords** CVD mixing rule · Gas adsorption · Multi-components · Prediction

**Notations**

| | |
|---|---|
| $a$ | specific molar volume of adsorbent, $m^2$/mol |
| $A$ | surface area per mass of adsorbent, $m^2$/kg |
| *%AAD* | percentage of absolute average deviation percent |
| $f$ | fugacity, Pa |
| $k$ | model constant, $10^{-5}$ mol/Pa·kg |
| $m$ | model constant in EOS and CVD mixing rule, dimensionless |
| $M$ | mass of adsorbent |
| $n$ | mole of components in adsorbed phase, mol |
| *NDP* | number of data points |
| $R$ | universal gas constant, Pa·$m^3$/mol·K |
| $T$ | temperature, K |
| $U$ | model coefficient, dimensionless |
| $W$ | model coefficient, dimensionless |
| $x$ | mole fraction in adsorbed phase, dimensionless |
| $y$ | mole fraction in gas phase, dimensionless |
| $Z$ | compressibility factor of adsorbed phase, dimensionless |
| $\alpha$ | EOS model constant, $10^{-1}$ Pa·$m^3$·kg/$mol^2$ |
| $\beta$ | EOS model constant, kg/mol |
| $\phi$ | fugacity coefficient, dimensionless |
| $\pi$ | spreading pressure, Pa·m |
| $\sigma$ | gas collision or Leonard-Jones diameter, Å |
| $\omega$ | mole adsorbed per mass of adsorbent, mol/kg |

**Superscripts**

| | |
|---|---|
| $a$ | adsorbed phase |
| *cal* | calculated |
| *exp* | experimental |
| $g$ | gas phase |

**Subscripts**

| | |
|---|---|
| $i$, $j$ | components $i$, $j$ in mixture |
| $LJ$ | Leonard-Jones |

## 1 Introduction

Adsorption offers an efficient tool dealing with separation of gaseous mixtures composed of small to moderate sized molecules. Multi-component adsorption data are vital information for designing an adsorption based separation process. It is preferable to estimate the multi-component adsorption equilibrium on the basis of the pure component adsorption isotherms. Various models have been proposed in the literature to predict the phase behavior of the gaseous mixtures adsorption. While a number of models have been developed for this purpose, prediction of the multi-component adsorption is still remaining a challenge (Craig and Seaton 1997). The most important models are as follow: the extended Langmuir model (Wojciechowski et al. 1985), the loading ratio correlation model (Ruthven 1984; Yang 1987; Perry and Chilton 1973), the ideal adsorption solution theory of Myers and Prausnitz (1965), the Flory-Huggins vacancy solution model (Suwanayuen and Danner 1980a, 1980b; Cochran et al. 1985), the model based on micropore size distribution and the extended Langmuir equation (Hu and Do 1996; Wang and Do 1997; Hu 1999; Qiao et al. 2000a), and the model based on micropore size distribution and the ideal adsorption solution theory (Qiao et al. 2000b; Wang et al. 2000).

Equations of state (EOS) are customarily utilized in order to predict the liquid-vapor equilibrium. Although to enhance the accuracy of the predictions, an EOS is used for the vapor phase and an activity coefficient model for the liquid phase (Pongsiri and Viswanath 1989). Inspired from above, Zhou et al. (1994) proposed a general two dimensional (2-D) EOS and the corresponding fugacity expression for the adsorbed phase to model the gas adsorption equilibrium. They showed that 2-D EOSs are interestingly capable to fit the pure adsorption isotherms accurately. In order to predict the multi-component adsorption equilibrium with a reasonable degree of accuracy, it is necessary to combine pure component constants, by the aid of a mixing rule prior to be used by any EOS. Accordingly, they demonstrated that 2-D EOSs utilizing classical or van der Waals (VDW) mixing rule, can be used to predict gaseous mixtures adsorption equilibrium. Cubic EOSs are the most widely used with the classical mixing rule (Novenario et al. 1996). A general review of the various mixing rules reveals that any improvement over the classical mixing rules is achieved at the cost of increase in the number of adjustable parameters (Mukhopadhyay and Rao 1993). However, this added complexity is not fully justified in that the uncertainty of one parameter is forced upon the others during regression. Moreover the calculated compositions are still extremely sensitive to the regressed binary interaction parameters (Mukhopadhyay and Rao 1993). Accordingly for the purpose of restricting the number of adjustable parameters to one and reducing their sensitivity as well, Rao developed a covolume-dependent (CVD) mixing rule (Rao and Mukhopadhyay 1988). This was revealed from the philosophy that, in a dilute supercritical mixture comprising molecules having large size differences, the probability of a molecule interacting with another in its immediate neighborhood depends on what fraction of its surface can be "seen" by the other molecule, regardless of its relative number or concentration. Furthermore, the repulsive forces become substantially important for the large sized molecules as a result of higher interaction energy. Hence in the CVD mixing rule, a covolume ($\beta_{ij}$) dependency has been introduced for the attraction energy parameter $\alpha_{ij}$ in order to account for the asymmetry and non-randomness. The ability of the original CVD mixing rule has been amply shown for pure solid-fluid binaries (Mukhopadhyay and Rao 1993; Rao and Mukhopadhyay 1989). Therefore, in the present work the range of applicability of CVD mixing rule is extended to the adsorption equilibrium possessing multi-component systems.

In this study, the general form of 2-D EOS is incorporated with the expression for the fugacity coefficient of the components using CVD mixing rule. In order to establish equilibrium relations between the adsorbed phase and the gas phase, the fugacity equation corresponding to the adsorbed phase is derived. Four well known forms of 2-D cubic EOSs: (1) van der Waals (VDW), (2) Soave-Redlich-Kwong (SRK), (3) Peng-Robinson (PR) and (4) Eyring, for five cases of multi-component gas adsorption systems extracted from the available open literature are evaluated. For all the EOSs, the predicted results using CVD mixing rule and classical mixing rule are compared to the aforementioned experimental data. To the best of our knowledge there is no documentation in the published literature associated with the application of the CVD mixing rule for the multi-component gas adsorption prediction.

## 2 The CVD mixing rule

In the present work, for the attraction energy parameter $a$ of the cubic EOS a CVD mixing rule which incorporates the concept of density dependence of cohesive energy parameter is proposed. In the original CVD mixing rule, the degree (or the exponent) of covolume dependency is uniform for both like and unlike interactions. Based on the preliminary calculations with various form of CVD mixing rule, we have

purposed a new (empirically based) CVD mixing rule as follow:

$$\alpha = \sum_i \sum_j x_i x_j \alpha_{ij} (\beta_{ij}/\beta)^{\theta} \tag{1}$$

It is necessary to recall that; however $\theta$ can be an adjustable parameter, even though here it is not an adjustable parameter, and it will be constant throughout this work and we run all the EOS models, in the conjunction with CVD mixing rule in the predictive mode only. Here, the covolume parameter $\beta$ is expressed by the conventional linear mixing rule:

$$\beta = \sum_i x_i \beta_{ii} \tag{2}$$

The other quantities in (1) are given as:

$$\alpha_{ij} = (\alpha_{ii} + \alpha_{jj})/2 \tag{3}$$

$$\beta_{ij} = \sqrt{\beta_{ii}.\beta_{jj}} \tag{4}$$

The generalized 2-D EOS is expressed as (Zhou et al. 1994; Do 1998):

$$\left[A\pi + \frac{\alpha\omega^2}{1 + U\beta\omega + W(\beta\omega)^2}\right][1 - (\beta\omega)^m] = \omega RT \tag{5}$$

where $A$ is the surface area per mass of adsorbent, $\pi$ is the spreading pressure, $\omega$ is the total amount adsorbed per mass adsorbent, $\alpha$ and $\beta$ are regressed model constants, $m$ is a parameter added for the model's flexibility, $R$ is the universal gas constant, and $T$ is temperature. The model coefficients, $U$, $W$, and $m$ must be specified to obtain a specific form of the 2-D EOS for application. For example, an analog of the VDW EOS is obtained by setting $m = 1$ and $U = W = 0$, similarly for the SRK ($m = U = 1$ and $W = 0$), the PR ($m = 1$, $U = 2$, and $W = -1$) and Eyring EOS ($m = 1/2$ and $U = W = 0$). Empirical parameter $\theta$ in this work was considered as 1 for all calculations.

## 3 Fugacity coefficient expression

The surface fugacity coefficient for a mixture components on the adsorbent surface can be calculated by the following thermodynamic equation (Zhou et al. 1994; Do 1998):

$$\ln \hat{\phi}_i^a = \int_0^{\omega} \left[\frac{1}{RT\omega}\left[\frac{\partial(A\pi)}{\partial\omega_i}\right]_{T,M_a,n_j} - \frac{1}{\omega}\right] d\omega - \ln Z_a \tag{6}$$

which $Z_a$, is defined by:

$$Z_a = \frac{a\pi}{RT} = \frac{A\pi}{RT\omega} \tag{7}$$

Substitution of (1), (2) and (5) into (6) and doing some stages of algebraic manipulations yields the fugacity expression in a general form for CVD mixing rule:

$$\ln \hat{\phi}_i^a = \frac{\beta_i \omega}{(\beta\omega)^{1-m} - \beta\omega} - \frac{1}{m}\ln[1 - (\beta\omega)^m] - \ln Z_a + T_1 + T_2 \tag{8}$$

Where

$$T_1 = -\frac{\alpha\beta_i\omega}{RT\beta[1 + U\beta\omega + W(\beta\omega)^2]} \tag{9}$$

$$T_2 = -\frac{\beta\psi_i - \alpha\beta_i\omega}{RT\beta^2\omega\sqrt{U^2 - 4W}} \times \ln\left[\frac{2 + \beta\omega(U + \sqrt{U^2 - 4W})}{2 + \beta\omega(U - \sqrt{U^2 - 4W})}\right] \tag{10}$$

$$\psi_i = 2\sum_{j=1}^{n} \omega_j \alpha_{ij} (\beta_{ij}/\beta)^{\theta} + \frac{2}{\omega}\sum_{\substack{j=1 \\ j\neq i}}^{n} \theta(\beta - \beta_i)\beta_{ij}^{\theta}\omega_i\omega_j\alpha_{ij}/\beta^{1+\theta} + \frac{1}{\omega}\theta(\beta - \beta_i)\beta_{ii}^{\theta}\omega_i\omega_i\alpha_{ii}/\beta^{1+\theta} \tag{11}$$

Clearly the value of $U$ and $W$ must satisfy the following constrains in the above fugacity expression:

$$U^2 - 4W > 0 \tag{12}$$

For the special case, $U = W = 0$; i.e. VDW and Eyring EOSs, the fugacity coefficient expression is simplified to:

$$\ln \hat{\phi}_i^a = \frac{\beta_i \omega}{(\beta\omega)^{1-m} - \beta\omega} - \frac{1}{m}\ln[1 - (\beta\omega)^m] - \ln Z_a - \frac{2}{RT}\sum_{j=1}^{n} \omega_j \alpha_{ij} (\beta_{ij}/\beta)^{\theta} - \frac{2}{RT\omega}\sum_{\substack{j=1 \\ j\neq i}}^{n} \theta(\beta - \beta_i)\beta_{ij}^{\theta}\omega_i\omega_j\alpha_{ij}/\beta^{1+\theta} - \frac{1}{RT\omega}\theta(\beta - \beta_i)\beta_{ii}^{\theta}\omega_i\omega_i\alpha_{ii}/\beta^{1+\theta} \tag{13}$$

## 4 Modeling of adsorption equilibria

The following equation holds at the equilibrium between the adsorbed phase and the gas phase:

$$Ax_i\pi\hat{\phi}_i^a = k_i RT \hat{f}_i^g \tag{14}$$

**Table 1** Case studies considered evaluating the CVD and the classical mixing rules

| Case | Components | Temperature (K) | Pressure (kPa) | References |
|---|---|---|---|---|
| A | $CO_2$, $C_2H_4$, $C_3H_8$ | 293 | Up to 100 | Calleja et al. (1998) |
| B | $H_2$, $N_2$, $CH_4$ | 283 and 298 | Up to 600 | Wu et al. (2005) |
| C | $CH_4$, $C_2H_4$, $C_2H_6$ | 301.4 | Up to 3500 | Myers and Prausnitz (1965) |
| D | $CO_2$, $C_2H_4$, $iC_4H_{10}$ | 298.15 and 323 | Up to 137.84 | Hyun and Daner (1982) |
| E | $CH_4$, $C_2H_6$, $nC_4H_{10}$ | 308, 353, 423 | Up to 268.6 | Gumma (2003) |

where $f_i^g$ is the gas fugacity calculated by the Soave–Redlich-Kwong SRK EOS; not shown here, for its simplicity and accuracy, $k_i$ is the model constant, denoting the slope of the pure component isotherm at the origin. Supplied with experimental adsorption data for pure $i$. The above equilibrium relation (14) combined with fugacity equation (8) for the adsorbed and fugacity equation of the gas phase for component $i$ can be utilized to obtain the models pure constants $\alpha_i$, $\beta_i$, and $k_i$. Thus, for pure substances, the EOS is a "three-parameter" model.

Pure substance constants for the 2-D EOS models are determined by minimizing the following objective function:

$$\%AAD = \frac{100}{NDP}\sum_{j=1}^{NDP}\left|\frac{\omega^{cal}(j)-\omega^{\exp}(j)}{\omega^{\exp}(j)}\right| \tag{15}$$

The percentage of absolute average deviations is carried out over entire data points for every pure component or mixture at a particular temperature. Applying pure substance parameters and selected mixing rules along with the fugacity coefficient equations by the aid of auxiliary equilibrium relations, result in attaining the adsorption of the individual components in a gaseous mixture. The algorithm for calculating the multi-component adsorption is as following (Peng et al. 2006):

(1) Parameters $\alpha_i$ and $\beta_i$, in (3) and (4), and $k_i$ in (14) for pure components are determined by fitting the experimental isotherms for pure components using a non linear regression algorithm.
(2) Initial value of total adsorption amount, $\omega^{cal}$, and compositions $x_i$, in the adsorbed phase are guessed.
(3) Parameters $\alpha_{ij}$ and $\beta_{ij}$ for the binary mixture are calculated from (3) and (4). Then, $\alpha$ and $\beta$ are evaluated from (1) and (2).
(4) $\omega^{cal}$ and $x_i$, are computed applying Newton's method coupled with Gaussian backward substitution method, to solve the nonlinear equations composed of (7), (8) and (14) simultaneously.

In summary, by using the aforementioned approach, the adsorption amount of the individual species can be solved from the total uptake of a mixture, where only the experimental data are available for total adsorbed amount. We recall that, in the case of multi-component adsorption predictions, combined with the classical mixing rule, (8) was replaced by the corresponding fugacity coefficient equations proposed by Zhou et al. (1994).

## 5 Case studies, results and discussions

In the present study, it was attempted that a variety of adsorbents and gas mixtures in wide range of temperatures and pressures to be considered. Five cases of multi-component gas adsorption systems extracted from the available open literature are evaluated. Authors note that the majority of these sets of data have not been already predicted using the 2-D EOS for multi-component adsorption, as shown in Table 1. The regressed pure component parameters are listed in Tables A1, A2, A3, A4 and A5, see Appendix.

Based on the concept of the CVD mixing rule explained by Rao and Mukhopadhyay (1988), that presents: "in a mixture comprising molecules having large *size differences*, the probability of a molecule interacting with another in its immediate neighborhood depends on what fraction of its surface can be seen by the other molecule regardless of its relative number or concentration, as a result, the repulsive forces become substantially important for the large sized molecules due to the higher interaction energy", it was inspired that CVD mixing rule could be a binding bridge between the *molecular size* and the *molecular interaction*; hence the interaction energy. Therefore, a glance on the *%AAD*s in Tables 3, 4, 5, 6 and 7 discloses this finding. To show this, the ratio of the classical mixing rule *%AAD* to the CVD mixing rule *%AAD* are plotted versus the difference of the collision or the Leonard-Jones diameters of the gas molecules in the mixtures, see Table 2 and Fig. 1. It is noted that, for the three components mixtures, first the diameter differences of the components; one by one, are computed, and then the arithmetic average among them is roughly calculated. Figure 1 shows the existence of a criterion between the CVD and the classical mixing rules in terms of molecular size difference. According to Fig. 1, $\Delta\sigma_{LJ} \approx 0.60$ Å is the criterion. The CVD mixing rule is approximately predominant in the region of $\Delta\sigma_{LJ} \geq 0.60$ Å, whilst, region of $\Delta\sigma_{LJ} \leq 0.60$ Å is nearly governed by the classical mixing rule. However there is not an exact and clear border between them, that's why, we can see for some of the cases the classical mixing rule is

**Table 2** Collision or Leonard-Jones diameters of the studied gases (Bae and Lee 2005; Semenova 2004)

| Gas | $H_2$ | $N_2$ | $CO_2$ | $CH_4$ | $C_2H_4$ | $C_2H_6$ | $C_3H_8$ | $iC_4H_{10}$ | $nC_4H_{10}$ |
|---|---|---|---|---|---|---|---|---|---|
| $\sigma_{LJ}$ (Å) | 2.93 | 3.68 | 4.0 | 3.82 | 4.29 | 4.42 | 5.06 | 5.34 | 5.34 |

**Table 3** Comparison of predictions for adsorption of $C_3H_8$, $C_2H_4$ and $CO_2$ at 293 K and 90 kPa, using CVD and classical mixing rule on ZSM-5 (Si/Al = 15) (Case A)

| Quantities | Points | CVD mixing rule | | | | Classical mixing rule | | | |
|---|---|---|---|---|---|---|---|---|---|
| | | VDW | SRK | PR | Eyring | VDW | SRK | PR | Eyring |
| | | $C_2H_4 + C_3H_8$, $\Delta\sigma_{LJ} = 0.77$ Å, *%AAD* | | | | | | | |
| $\omega_i$ | 36 | 27.13 | 28.74 | 34.66 | 32.86 | 40.81 | 35.50 | 42.94 | 73.54 |
| $\omega$ | 36 | 14.30 | 14.36 | 17.91 | 22.39 | 16.96 | 16.42 | 20.90 | 37.86 |
| | | $C_2H_4 + CO_2$, $\Delta\sigma_{LJ} = 0.29$ Å, *%AAD* | | | | | | | |
| $\omega_i$ | 36 | 14.69 | 7.29 | 10.01 | 43.50 | 11.33 | 7.24 | 9.07 | 26.28 |
| $\omega$ | 36 | 3.72 | 3.18 | 2.27 | 4.72 | 3.71 | 3.18 | 2.27 | 3.23 |
| | | $C_3H_8 + CO_2$, $\Delta\sigma_{LJ} = 1.06$ Å, *%AAD* | | | | | | | |
| $\omega_i$ | 36 | 22.18 | 23.88 | 40.60 | 24.12 | 29.05 | 27.68 | 44.75 | 37.70 |
| $\omega$ | 36 | 9.42 | 11.88 | 19.95 | 9.12 | 14.73 | 14.77 | 24.73 | 22.20 |
| | | $C_2H_4 + C_3H_8 + CO_2$, $\Delta\bar{\sigma}_{LJ} = 0.71$ Å, *%AAD* | | | | | | | |
| $\omega_i$ | 30 | 22.63 | 21.26 | 34.94 | 35.01 | 38.89 | 25.80 | 40.24 | 64.36 |
| $\omega$ | 30 | 14.15 | 14.96 | 21.48 | 20.35 | 22.18 | 16.94 | 24.38 | 39.40 |
| | | Overall, *%AAD* | | | | | | | |
| $\omega_i$ | 138 | 21.61 | 20.25 | 29.84 | 33.82 | 29.63 | 23.98 | 33.99 | 49.87 |
| $\omega$ | 138 | 10.23 | 10.93 | 15.14 | 13.88 | 14.06 | 12.65 | 17.80 | 25.08 |

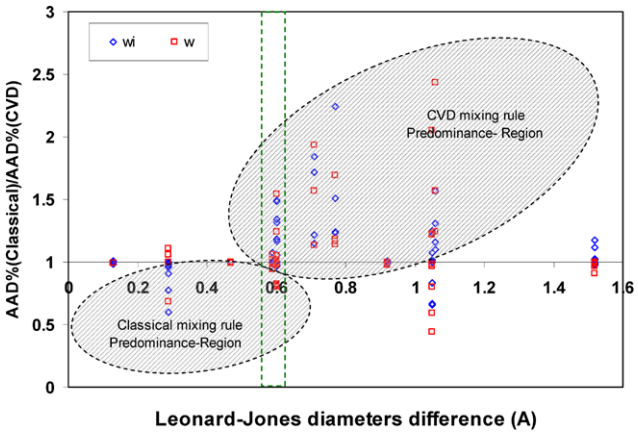


**Fig. 1** Ratio of the classical mixing rule *%AAD* to the CVD mixing rule *%AAD* versus Leonard-Jones diameters difference (Å)

located at the higher values of $\Delta\sigma_{LJ} \geq 0.6$ Å or vise versa for the CVD mixing rule, but the overall trends follow the criterion still.

The five selected case studies are as follows:

*Case A* $CO_2$, $C_2H_4$ and $C_3H_8$ binary and ternary adsorption on ZSM-5 Zeolite at 293 K and pressures up to 100 kPa which were reported by Calleja et al. (1998). The fitted parameters for the pure components are shown in Table A1. According to Table A1, the excellent ability of the all EOS models to describe the pure isotherms for propane and carbon dioxide can be realized, however for Ethylene show slightly higher amount of *%AAD*. Table 3 exhibits %AAD for the CVD and the classical mixing rules. Comparing the results from Table 3 to Fig. 1, it can be seen that for $\Delta\sigma_{LJ} = 0.29$ Å the classical mixing rule is predicting better than the CVD mixing rule, whilst for the rest systems; $\Delta\sigma_{LJ} \geq 0.60$ Å, the CVD mixing rule predicts the multicomponent adsorption substantially stronger than the classical mixing rule, including all of the EOS models. Typical prediction results are shown in Figs. 2, 3, 4 and 5. As can be seen from Fig. 2, since this system exhibits an azeotrope point on $x-y$ diagram, as a result it is known as a highly non ideal system. According to Fig. 2 clearly demonstrates that CVD mixing rule not only predicts much stronger relative to classical mixing rule, but also, has this ability to predict the systems showing non ideality as: $C_2H_4 + C_3H_8$. Figures 3, 4 and 5 express the ability of CVD mixing rule against classical mixing rule to predict the total amount adsorbed versus pressure. Obviously, the power of the CVD mixing rule over he classical mixing rule can be interpreted associated with the molecular size differences.

*Case B* $CH_4$, $N_2$ and $H_2$ ternary adsorption on activated carbon JX101 at temperatures of 283 and 298 K and pressures

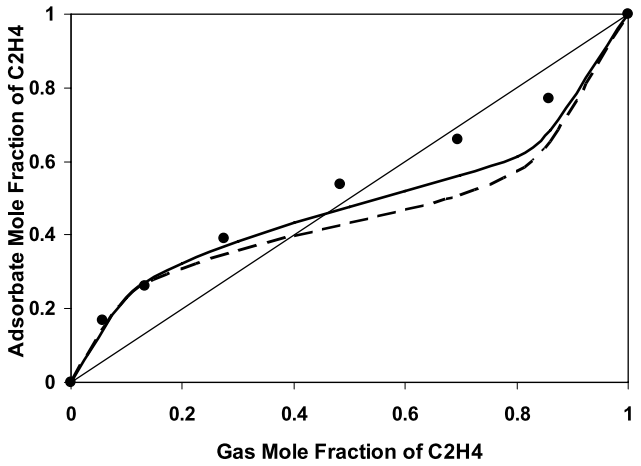


**Fig. 2** Predicted $x$–$y$ diagram for $C_2H_4$ in $C_2H_4 + C_3H_8$ at 293 K and 90 kPa, using SRK EOS with CVD mixing rule (*solid line*) and SRK EOS with classical mixing rule (*dashed line*), against experimental data (•) on ZSM-5 (Do 1998) (Case A)

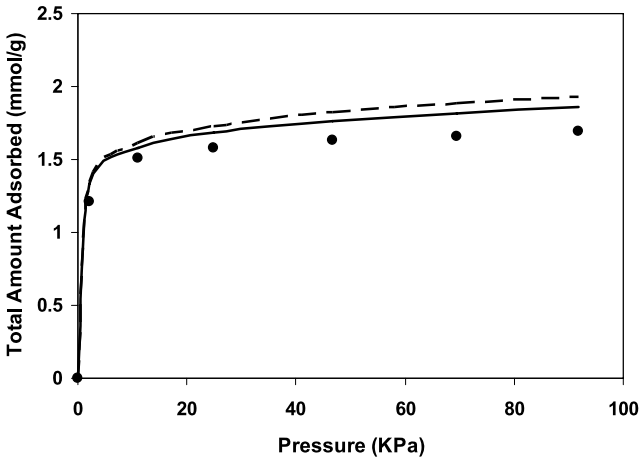


**Fig. 3** Predicted total amount adsorbed versus pressure for $CO_2 + C_3H_8$ at 293 K and $y_{CO_2} = 0.111$, using SRK EOS with CVD mixing rule (*solid line*) and SRK EOS with classical mixing rule (*dashed line*), against experimental data (•) on ZSM-5 (Do 1998) (Case A)

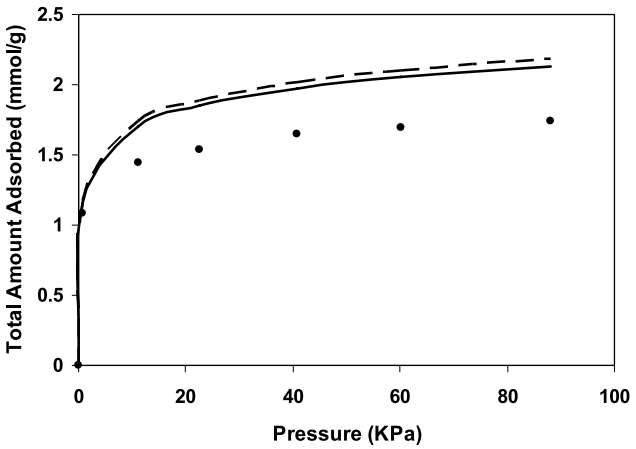


**Fig. 4** Predicted total amount adsorbed versus pressure for $C_2H_4 + C_3H_8$ at 293 K and $y_{CO_2} = 0.5$, using VDW EOS with CVD mixing rule (*solid line*) and VDW EOS with classical mixing rule (*dashed line*), against experimental data (•) on ZSM-5 (Do 1998) (Case A)

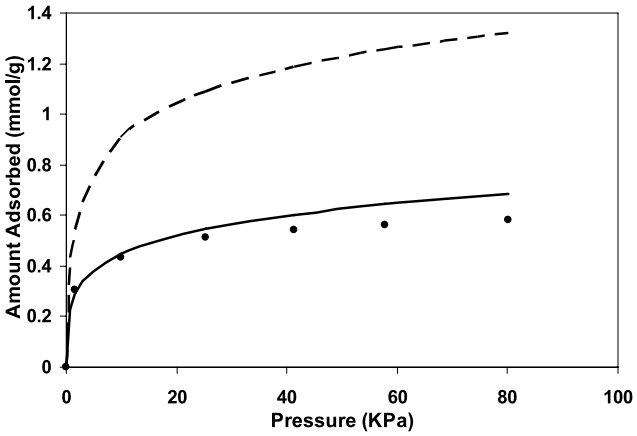


**Fig. 5** Predicted amount adsorbed of Ethylene versus pressure for $CO_2 + C_2H_4 + C_3H_8$ at 293 K and $y_{CO_2} = 0.1429/y_{C_2H_4} = 0.2857$, using VDW EOS with CVD mixing rule (*solid line*) and VDW EOS with classical mixing rule (*dashed line*), against experimental data (•) on ZSM-5 (Do 1998) (Case A)

to 600 kPa, which were reported by Wu et al. (2005). The EOS models parameters and predictions are presented in Tables A2 and 4 respectively. This system exhibits an ideal behavior, not shown here. Table 4 exhibits that CVD mixing rule and classical mixing rule are closely competing to predict the multi-component adsorption. Again, this can be interpreted in terms of the molecular size difference. The average $\Delta\sigma_{LJ} = 0.59$ Å, so overlaps with the criterion, that is $\approx 0.60$ Å. Because of this, the CVD and The classical mixing rules exhibit the same results equally. SRK and PR EOSs combined with the classical mixing rule predict better, while VDW and Eyring EOSs using CVD mixing rule are superior.

*Case C* $CH_4$, $C_2H_6$ and $C_2H_4$ binary adsorption on activated carbon at 301.4 K and pressures up to 3500 kPa which were reported by Reich et al. (1980). The regression and calculation results are presented in Tables A3 and 5 respectively. Parameters represented in Table A3 are from Zhou et al. (1994). This system has a symmetrical $x$–$y$ diagram, so it can be known as ideal system. According to Table 5, it is realized that, although, both mixing rules exhibit considerable ability to predict the multi-component adsorption, classical mixing rule shows marginally higher capability to describe the mixture adsorption. As can be seen from Fig. 6, both of them show high consistency with the experimental data. Again, this can be interpreted in terms of the molec-

**Table 4** Comparison of predictions for adsorption of $CH_4$,$N_2$ and $H_2$ at 283 and 298 K, using CVD and classical mixing rule on activated carbon (Case B)

| Quantities | Points | CVD mixing rule | | | | Classical mixing rule | | | |
|---|---|---|---|---|---|---|---|---|---|
| | | VDW | SRK | PR | Eyring | VDW | SRK | PR | Eyring |
| | | $CH_4 + N_2 + H_2$, $\Delta\bar{\sigma}_{LJ} = 0.59$ Å, *%AAD* | | | | | | | |
| $\omega_i$ | 54 | 18.12 | 18.03 | 19.02 | 37.14 | 18.27 | 17.72 | 18.87 | 39.86 |
| $\omega$ | 54 | 9.89 | 9.85 | 11.11 | 8.88 | 9.86 | 9.31 | 10.52 | 9.42 |

**Table 5** Comparison of predictions for adsorption of $CH_4$, $C_2H_6$ and $C_2H_4$ on activated carbon at 301.4 K, using CVD and classical mixing rule (Case C)

| Quantities | Points | CVD mixing rule | | | | Classical mixing rule | | | |
|---|---|---|---|---|---|---|---|---|---|
| | | VDW | SRK | PR | Eyring | VDW | SRK | PR | Eyring |
| | | $CH_4 + C_2H_6$, $\Delta\sigma_{LJ} = 0.60$ Å, *%AAD* | | | | | | | |
| $\omega_i$ | 12 | 15.88 | 17.69 | 18.13 | 18.96 | 16.75 | 17.56 | 18.10 | 18.93 |
| $\omega$ | 12 | 5.54 | 6.06 | 6.19 | 6.46 | 5.41 | 5.95 | 6.13 | 6.45 |
| | | $CH_4 + C_2H_4$, $\Delta\sigma_{LJ} = 0.47$ Å, *%AAD* | | | | | | | |
| $\omega_i$ | 15 | 17.78 | 18.16 | 18.42 | 18.63 | 17.76 | 18.22 | 18.48 | 18.69 |
| $\omega$ | 15 | 5.91 | 6.24 | 6.30 | 6.36 | 5.90 | 6.21 | 6.29 | 6.36 |
| | | $C_2H_6 + C_2H_4$, $\Delta\sigma_{LJ} = 0.13$ Å, *%AAD* | | | | | | | |
| $\omega_i$ | 12 | 5.15 | 5.20 | 5.19 | 5.29 | 5.20 | 5.23 | 5.21 | 5.22 |
| $\omega$ | 12 | 5.36 | 5.40 | 5.41 | 5.43 | 5.32 | 5.36 | 5.37 | 5.37 |
| | | Overall, *%AAD* | | | | | | | |
| $\omega_i$ | 39 | 13.31 | 14.03 | 14.26 | 14.63 | 13.58 | 14.02 | 14.28 | 14.62 |
| $\omega$ | 39 | 5.63 | 5.93 | 5.99 | 6.10 | 5.57 | 5.87 | 5.96 | 6.08 |

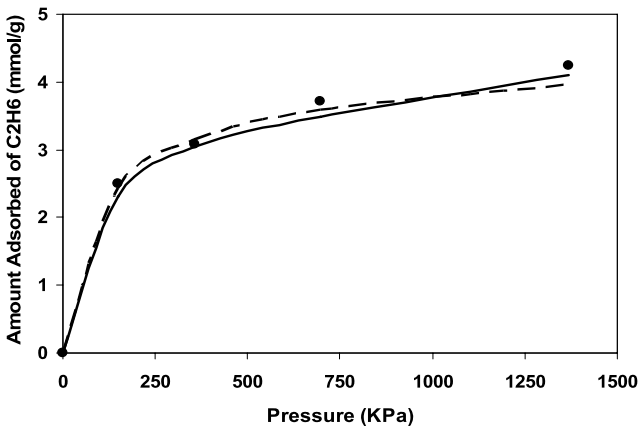


**Fig. 6** Predicted amount adsorbed of Ethylene versus pressure for $CH_4 + C_2H_4$ at 301.4 K and $y_{CH_4} = 0.682$, using PR EOS with CVD mixing rule (*solid line*) and PR EOS with classical mixing rule (*dashed line*), against experimental data (•) on activated carbon (Calleja et al. 1998) (Case C)

ular size difference. The molecular size differences are less than 0.60 Å, that is the criterion. Because of this, in general, the classical mixing rules exhibit slightly better results than CVD mixing rule.

*Case D* $CO_2$, $C_2H_4$ and $iC_4H_{10}$ binary adsorption on 13X molecular sieve at 298.15 and 323 K and pressure up to 137.84 kPa which were presented by Hyun and Daner (1982). The systems of $CO_2 + C_2H_4$ at 298.15 K and $iC_4H_{10} + C_2H_4$ at 298.15 and 323.15 K were considered to evaluate the mixing rules. These are highly non ideal systems, since they exhibit azeotropic behavior on the $x$–$y$ diagram. Table A4, shows the pure substance model parameters. These parameters were obtained from Zhou et al. (1994). Comparing the results from Table 6 to Fig. 1, it can be seen that for the system of $CO_2 + C_2H_4$, $\Delta\sigma_{LJ} = 0.29 < 0.6$ Å thus, the classical mixing rule is predicting marginally better than the CVD mixing rule, whilst for the system of $iC_4H_{10} + C_2H_4$ at 298 K; $\Delta\sigma_{LJ} = 1.05 \geq 0.60$ Å, the CVD mixing rule predicts the multi-component adsorption stronger than the classical mixing rule. Although, for the system of $C_2H_4 + iC_4H_{10}$ at 323 K where $\Delta\sigma_{LJ} = 1.52 > 0.6$ Å, the classical mixing rule is superior. This is an exception to what we explained in terms of the molecular size differences. This shows that, even though the molecular size differences exhibit a strong binding with CVD mixing rule, likely the other factors such as concentration and temperature should be taken into consideration as well. Generally speaking, the CVD mixing rule has the capability to predict the systems of non ideal mixture suitably; these are shown in $x$–$y$ diagrams of Figs. 7 and 8.

**Table 6** Comparison of predictions for adsorption of $CO_2$, $C_2H_4$ and $iC_4H_{10}$ on 13X molecular sieve at 298 and 323 K, using CVD and classical mixing rule (Case D)

| Quantities | Points | CVD mixing rule | | | | Classical mixing rule | | | |
|---|---|---|---|---|---|---|---|---|---|
| | | VDW | SRK | PR | Eyring | VDW | SRK | PR | Eyring |
| | | $CO_2 + C_2H_4$ at 298 K, $\Delta\sigma_{LJ} = 0.29$ Å, *%AAD* | | | | | | | |
| $\omega_i$ | 6 | 21.59 | 17.78 | 17.52 | 23.70 | 21.15 | 17.06 | 16.89 | 23.61 |
| $\omega$ | 6 | 10.63 | 8.75 | 8.77 | 8.26 | 10.62 | 9.29 | 9.25 | 9.17 |
| | | $C_2H_4 + iC_4H_{10}$ at 298 K, $\Delta\sigma_{LJ} = 1.05$ Å, *%AAD* | | | | | | | |
| $\omega_i$ | 10 | 11.11 | 11.47 | 12.31 | 22.87 | 11.91 | 14.36 | 15.22 | 23.28 |
| $\omega$ | 10 | 2.16 | 2.74 | 2.30 | 1.32 | 2.63 | 1.21 | 1.37 | 2.71 |
| | | $C_2H_4 + iC_4H_{10}$ at 323 K, $\Delta\sigma_{LJ} = 1.05$ Å, *%AAD* | | | | | | | |
| $\omega_i$ | 8 | 6.52 | 7.06 | 7.06 | 7.95 | 5.41 | 4.68 | 4.67 | 7.96 |
| $\omega$ | 8 | 2.30 | 2.38 | 2.42 | 2.78 | 2.82 | 2.35 | 2.33 | 2.23 |
| | | Overall, *%AAD* | | | | | | | |
| $\omega_i$ | 24 | 12.2 | 11.58 | 11.86 | 18.10 | 12.05 | 11.80 | 12.12 | 18.26 |
| $\omega$ | 24 | 4.68 | 4.37 | 4.23 | 3.83 | 5.02 | 3.95 | 3.99 | 4.43 |

**Table 7** Comparison of predictions for adsorption of $CH_4$, $C_2H_6$ and $nC_4H_{10}$ at 308–423 K, using CVD and classical mixing rule on silicalite (Case E)

| Quantities | Points | CVD mixing rule | | | | Classical mixing rule | | | |
|---|---|---|---|---|---|---|---|---|---|
| | | VDW | SRK | PR | Eyring | VDW | SRK | PR | Eyring |
| | | $CH_4 + C_2H_6$, Case 1, $\Delta\sigma_{LJ} = 0.60$ Å, *%AAD* | | | | | | | |
| $\omega_i$ | 5 | 7.51 | 5.75 | 5.76 | 4.53 | 7.27 | 6.80 | 6.72 | 6.76 |
| $\omega$ | 5 | 2.02 | 2.83 | 2.91 | 2.75 | 2.06 | 2.29 | 2.41 | 3.42 |
| | | $CH_4 + C_2H_6$, Case 2, $\Delta\sigma_{LJ} = 0.60$ Å, *%AAD* | | | | | | | |
| $\omega_i$ | 12 | 8.38 | 6.88 | 6.76 | 6.82 | 8.15 | 9.24 | 8.92 | 10.09 |
| $\omega$ | 12 | 1.25 | 2.12 | 2.21 | 1.85 | 1.31 | 1.70 | 1.80 | 2.85 |
| | | $C_2H_6 + nC_4H_{10}$, Case 1, $\Delta\sigma_{LJ} = 0.92$ Å, *%AAD* | | | | | | | |
| $\omega_i$ | 3 | 40.29 | 35.77 | 31.91 | 48.76 | 40.48 | 35.53 | 31.69 | 48.78 |
| $\omega$ | 3 | 8.67 | 5.29 | 5.59 | 7.58 | 8.68 | 5.22 | 5.51 | 7.59 |
| | | $C_2H_6 + nC_4H_{10}$, Case 2, $\Delta\sigma_{LJ} = 0.92$ Å, *%AAD* | | | | | | | |
| $\omega_i$ | 5 | 41.24 | 38.17 | 34.28 | 50.46 | 41.47 | 37.78 | 33.86 | 50.48 |
| $\omega$ | 5 | 4.97 | 3.31 | 3.26 | 4.96 | 4.98 | 3.22 | 3.17 | 4.96 |
| | | $CH_4 + nC_4H_{10}$, at 308 K, $\Delta\sigma_{LJ} = 1.52$ Å, *%AAD* | | | | | | | |
| $\omega_i$ | 13 | 27.11 | 14.77 | 14.71 | 45.22 | 30.35 | 14.82 | 17.32 | 46.23 |
| $\omega$ | 13 | 7.16 | 4.08 | 4.58 | 5.53 | 7.17 | 4.00 | 4.49 | 5.53 |
| | | $CH_4 + nC_4H_{10}$, at 353 K, $\Delta\sigma_{LJ} = 1.52$ Å, *%AAD* | | | | | | | |
| $\omega_i$ | 10 | 41.7 | 42.51 | 42.77 | 30.62 | 41.73 | 42.54 | 42.81 | 30.39 |
| $\omega$ | 10 | 5.53 | 5.56 | 5.57 | 5.01 | 5.53 | 5.56 | 5.57 | 4.54 |
| | | $CH_4 + nC_4H_{10}$, at 423 K, $\Delta\sigma_{LJ} = 1.52$ Å, *%AAD* | | | | | | | |
| $\omega_i$ | 10 | 39.71 | 40.48 | 40.52 | 36.81 | 40.41 | 39.71 | 39.82 | 35.81 |
| $\omega$ | 10 | 18.10 | 17.88 | 17.97 | 21.16 | 18.07 | 17.66 | 17.78 | 20.5 |
| | | Overall, *%AAD* | | | | | | | |
| $\omega_i$ | 58 | 28.13 | 24.68 | 24.16 | 30.44 | 28.95 | 25.09 | 25.11 | 31.32 |
| $\omega$ | 58 | 6.99 | 6.20 | 6.36 | 7.19 | 7.00 | 6.00 | 6.17 | 7.26 |

**Table 8** Overall comparison of predictions for adsorption considering the total data, using CVD and classical mixing rule

| Quantities | Points | CVD mixing rule | | | | Classical mixing rule | | | |
|---|---|---|---|---|---|---|---|---|---|
| | | VDW | SRK | PR | Eyring | VDW | SRK | PR | Eyring |
| | | Gross overall, *%AAD* | | | | | | | |
| $\omega_i$ | 313 | 20.46 | 19.25 | 23.60 | 30.17 | 24.20 | 20.93 | 25.60 | 37.89 |
| $\omega$ | 313 | 8.57 | 8.74 | 10.84 | 12.89 | 10.28 | 9.33 | 11.85 | 15.13 |

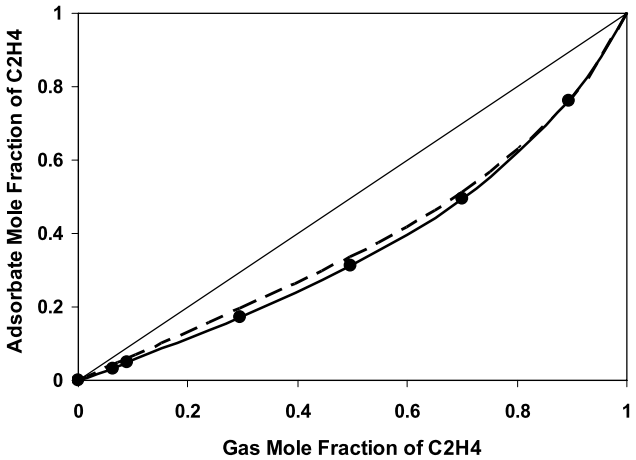


**Fig. 7** Predicted $x-y$ diagram for ethylene in $CO_2+C_2H_4$ at 298.15 K and 138 kPa, using SRK EOS with CVD mixing rule (*solid line*) and SRK EOS with classical mixing rule (*dashed line*), against experimental data (•) on 13X molecular sieve (Wu et al. 2005) (Case D)

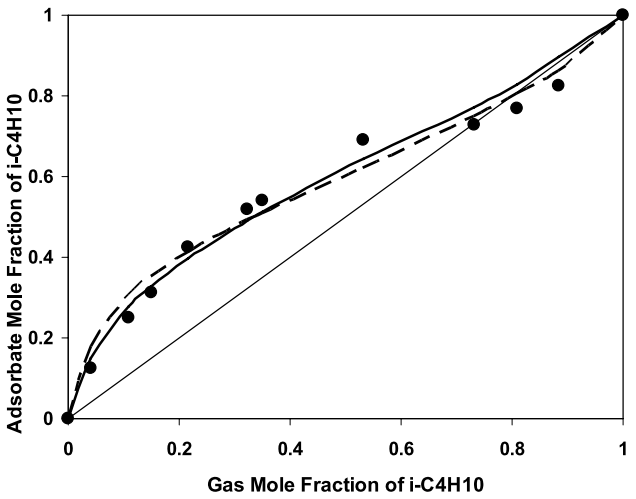


**Fig. 8** Predicted $x-y$ diagram for $iC_4H_{10}$ in $C_2H_4+iC_4H_{10}$ at 298.15 K and 138 kPa, using SRK EOS with CVD mixing rule (*solid line*) and SRK EOS with classical mixing rule (*dashed line*), against experimental data (•) on 13X molecular sieve (Wu et al. 2005) (Case D)

*Case E* $CH_4$, $C_2H_6$ and $nC_4H_{10}$ binary adsorption of $CH_4+C_2H_6$ and $C_2H_6+nC_4H_{10}$ at 308 K and $CH_4+nC_4H_{10}$ at 308, 353 and 423 K on Silicalite up to 268.6 kPa which were reported by Gumma (2003). The results of the EOS models parameters and predictions are presented in

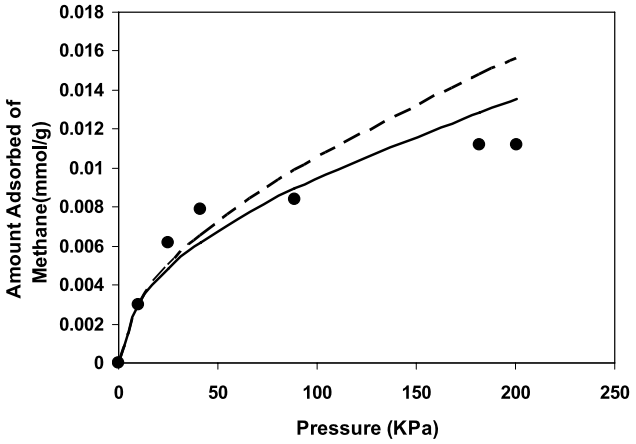


**Fig. 9** Predicted amount adsorbed of methane versus pressure for $CH_4+nC_4H_{10}$ at 308 K and $y_{CH_4}=0.891$, using PR EOS with CVD mixing rule (*solid line*) and PR EOS with classical mixing rule (*dashed line*), against experimental data (•) on silicalite (Reich et al. 1980) (Case E)

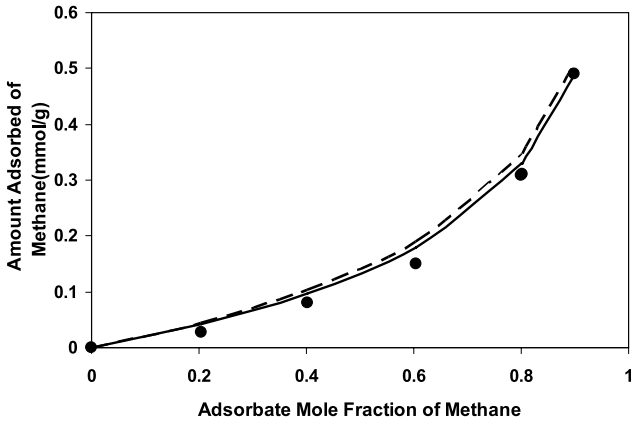


**Fig. 10** Predicted amount adsorbed of methane versus bulk methane mole fraction for $CH_4+nC_4H_{10}$ at 308 K and 268 kPa, using Eyring EOS with CVD mixing rule (*solid line*) and Eyring EOS with classical mixing rule (*dashed line*), against experimental data (•) on silicalite (Reich et al. 1980) (Case E)

Tables A5 and 7 respectively. All EOS models, exhibit high accuracy to predict the pure components isothermal adsorption. Considering Table 7, predictions of $CH_4+C_2H_6$ at 308 K and $CH_4+nC_4H_{10}$ at 308 and 353 K, are predominated by CVD mixing rule rather than classical mixing rule. Figure 9 shows the amount adsorbed versus pressure mean-

while Fig. 10 exhibits the amount adsorbed versus gas phase mole fraction for Methane applying both CVD and classical mixing rule. Obviously the CVD mixing rule predictions are more consistent with the experimental data shown on the figures. However at some conditions the classical mixing predicts with the same degree of accuracy as the CVD mixing rule. Again, this can be explained in terms of the molecular size difference. The molecular size differences are $\geq 0.60$ Å. Because of this, in general, the CVD mixing rules exhibit better results than classical mixing rule. For the case: $C_2H_6 + nC_4H_{10}$ at 308 K both CVD and classical mixing rule exhibit considerable and equal ability to estimate the multi-component adsorption. For example SRK and PR EOSs for the classical mixing rule are superior while VDW and Eyring EOSs using the CVD mixing rule are predominated. This can be interpreted in terms of the molecular size difference as well. As we presented previously, there is no a clear border concerned with the molecular size differences, that's why, even at $\Delta\sigma_{LJ} = 0.92 > 0.60$ Å, the CVD and the classical mixing rules exhibit the degree of accuracy. However, in some cases, i.e. $CH_4 + nC_4H_{10}$ at 423 K that $\Delta\sigma_{LJ} = 1.52$ Å, the classical mixing rule is again slightly better. This is also an exception to what we explained in terms of the molecular size differences.

## 6 Conclusion

CVD mixing rule was suitably developed to predict the multi-component gas adsorption equilibrium. The general form of 2-D EOS was incorporated into the derivation of the fugacity coefficient equation using CVD mixing rule. To the best of our knowledge there is no documentation in the published literature associated with the application of the CVD mixing rule for the multi-component gas adsorption prediction. Hence, this form of fugacity coefficient equation has not been observed in the literature. Four 2-D EOS models were evaluated against five cases of the gas adsorption systems in the predictive mode. To examine the CVD mixing rule, several binary and ternary gas mixtures covering ideal and non-ideal systems were considered. The correlated pure component parameters were applied to predict multi-component adsorption, for both the CVD and the classical mixing rule. For all the gaseous mixtures used in our case studies, the predicted results from the CVD mixing rule and the classical mixing rule were compared with the experimental data. Based on the concept of the CVD mixing rule explained by Rao and Mukhopadhyay (1988), it was inspired that CVD mixing rule could be a binding bridge between the *molecular size* and the *molecular interaction*; hence the interaction energy. To show this, the ratio of the classical mixing rule *%AAD* to the CVD mixing rule *%AAD* were plotted versus the difference of the collision or the Leonard-Jones diameters of the gas molecules in the mixtures. Figure 1 shows that there is a criterion between the CVD and the classical mixing rules in terms of molecular size difference. According to Fig. 1, $\Delta\sigma_{LJ} \approx 0.60$ Å is the criterion. The CVD mixing rule is approximately predominant in the region of $\Delta\sigma_{LJ} \geq 0.60$ Å, whilst, region of $\Delta\sigma_{LJ} \leq 0.60$ Å is nearly governed by the classical mixing rule. However there is not an exact and clear border between them, that's why, we can see for some of the cases the classical mixing rule is located at the higher values of $\Delta\sigma_{LJ} \geq 0.6$ Å or vise versa for the CVD mixing rule, but the overall trends follow the criterion. Generally speaking, as Table 8 exhibits, it seems that CVD mixing rule can be a strong tool to predict multi-component adsorption of gaseous mixtures. Among four EOS models we have tested, SRK and VDW EOS models with CVD mixing rule are more accurate for multi-component gas adsorption systems and then followed by PR and Eyring EOS models. The same trend can be realized for the classical mixing rule as well. It is expected that the 2-D EOS model with CVD mixing rule can be refined to enhance the results provided that parameter '$\theta$' in the CVD mixing rule, to be regressed, which in this case it is known as correlative mode. It seems that the ability of various mixing rules to attain an accurate and reliable prediction, directly dependents on the behavior of the multi-component systems. Finally, it seems that application of the CVD mixing rule predicting the adsorption of the multi-component systems needs much more investigation on various adsorbents and conditions.

## Appendix

**Table A1** Regression results for adsorption of $C_3H_8$, $C_2H_4$ and $CO_2$ on Zeolite at 293 K (Case A)

| Model | $\alpha_i$ | $\beta_i$ | Ln($k_i$) | *%AAD* |
|---|---|---|---|---|
| | | Propane at 293 K | | |
| SRK | −21401.2 | 0.4965 | 8.6263 | 1.17 |
| PR | −21193.6 | 0.4973 | 8.4653 | 1.18 |
| VDW | −22176.4 | 0.4795 | 9.0159 | 1.19 |
| Eyring | 4842.57 | 0.4355 | 9.3285 | 1.25 |
| | | Ethylene at 293 K | | |
| SRK | −57197.7 | 0.1506 | 8.9274 | 4.05 |
| PR | −59792.8 | 0.1234 | 8.6007 | 3.91 |
| VDW | −49297.9 | 0.0425 | 8.5985 | 4.62 |
| Eyring | −49132.7 | 0.0025 | 8.6249 | 4.60 |
| | | Carbon dioxide at 293 K | | |
| SRK | −46179.5 | 0.1583 | 8.0696 | 2.10 |
| PR | −49849.7 | 0.1036 | 8.0821 | 1.83 |
| VDW | −36518.2 | 0.0840 | 7.4889 | 2.31 |
| Eyring | −30242.6 | 0.0616 | 7.5139 | 2.20 |

**Table A2** Regression results for adsorption of $CH_4$, $N_2$ and $H_2$, on activated carbon at 283 and 298 K (Case B)

| Model | $\alpha_i$ | $\beta_i$ | Ln($k_i$) | *%AAD* |
|---|---|---|---|---|
| | | Nitrogen at 283 K | | |
| SRK | −2527.3 | 0.0297 | −0.8514 | 0.84 |
| PR | −2646.1 | 0.0297 | −0.8469 | 0.76 |
| VDW | −2466.3 | 0.0297 | −0.8514 | 0.96 |
| Eyring | 450.7 | 0.0255 | −0.6422 | 0.88 |
| | | Nitrogen at 298 K | | |
| SRK | 1145.2 | 0.1191 | −1.2850 | 2.37 |
| PR | 105.9 | 0.0980 | −1.2568 | 2.38 |
| VDW | −1097.9 | 0.0587 | −1.2534 | 2.44 |
| Eyring | 8146.4 | 0.1036 | −0.8936 | 5.50 |
| | | Hydrogen at 283 K | | |
| SRK | −1327.7 | 0.0173 | −3.2320 | 4.39 |
| PR | −1098.8 | 0.0271 | −3.2321 | 4.39 |
| VDW | −1181.0 | 0.0231 | −3.2321 | 4.39 |
| Eyring | −1855.7 | 0.0002 | −3.2081 | 4.52 |
| | | Hydrogen at 298 K | | |
| SRK | 2153.7 | 0.0524 | −3.4712 | 2.25 |
| PR | 1747.3 | 0.0404 | −3.4699 | 2.25 |
| VDW | 7260.2 | 0.2540 | −3.4706 | 2.21 |
| Eyring | 24053.7 | 0.1510 | −3.2565 | 3.73 |
| | | Methane at 283 K | | |
| SRK | −2568.2 | 0.0484 | 0.5317 | 0.52 |
| PR | −2846.0 | 0.0506 | 0.5577 | 0.52 |
| VDW | −3518.9 | 0.0014 | 0.5194 | 0.52 |
| Eyring | −3171.1 | 0.0011 | 0.5974 | 0.56 |
| | | Methane at 298 K | | |
| SRK | −1174.3 | 0.0748 | 0.0255 | 2.39 |
| PR | −2878.2 | 0.0305 | 0.0305 | 3.26 |
| VDW | −1013.2 | 0.0741 | 0.0207 | 2.35 |
| Eyring | −2814.7 | 0.0010 | 0.1013 | 3.38 |

**Table A3** Pure component parameters for adsorption of $CH_4$, $C_2H_6$ and $C_2H_4$, on activated carbon at 301.4 K (Case C, correlations were done by Zhou et al. 1994)

| Model | $\alpha_i$ | $\beta_i$ | Ln($k_i$) |
|---|---|---|---|
| | Methane | | |
| SRK | −2896.0 | 0.0710 | −0.2580 |
| PR | −3003.0 | 0.0772 | −0.2479 |
| VDW | −3493.0 | 0.0404 | −0.2649 |
| Eyring | −4043.0 | 0.0880 | 0.1696 |
| | Ethane | | |
| SRK | −3909.0 | 0.1080 | 2.5210 |
| PR | −4689.0 | 0.1075 | 2.5630 |
| VDW | −3073.0 | 0.1030 | 2.4470 |
| Eyring | 1885.0 | 0.0913 | 3.0210 |
| | Ethylene | | |
| SRK | −4802.0 | 0.0923 | 2.2200 |
| PR | −5678.0 | 0.0921 | 2.2710 |
| VDW | −4110.0 | 0.0813 | 2.1460 |
| Eyring | 0.4 | 0.7601 | 2.6820 |

**Table A4** Pure component parameters for adsorption of $CO_2$, $C_2H_4$ and $iC_4H_{10}$, on 13X molecular sieve at 298 and 323 K (Case D, correlations were done by Zhou et al. 1994)

| Model | $\alpha_i$ | $\beta_i$ | Ln($k_i$) |
|---|---|---|---|
| | Isobutane at 298 K | | |
| SRK | −16670.0 | 0.4406 | 7.9030 |
| PR | −20190.0 | 0.4385 | 7.9580 |
| VDW | −10930.0 | 0.4359 | 7.7380 |
| Eyring | 14830.0 | 0.3976 | 8.0420 |
| | Ethylene at 298 K | | |
| SRK | −12450.0 | 0.2118 | 5.4760 |
| PR | −14640.0 | 0.2107 | 5.5250 |
| VDW | −10680.0 | 0.1878 | 5.4110 |
| Eyring | 0.4 | 0.1783 | 5.8880 |
| | Carbon dioxide at 298 K | | |
| SRK | −13090.0 | 0.0822 | 5.6390 |
| PR | −14820.0 | 0.0890 | 5.7110 |
| VDW | −13220.0 | 0.0010 | 5.5490 |
| Eyring | −7325.0 | 0.0571 | 5.9070 |
| | Isobutane at 323 K | | |
| SRK | −2609.0 | 0.4919 | 6.1870 |
| PR | −2989.0 | 0.4918 | 6.1880 |
| VDW | −1399.0 | 0.4919 | 6.1500 |
| Eyring | 25740.0 | 0.4419 | 6.6640 |
| | Ethylene at 323 K | | |
| SRK | −9028.0 | 0.2111 | 3.9720 |
| PR | −10320.0 | 0.2126 | 3.9930 |
| VDW | 8230.0 | 0.1878 | 3.9440 |
| Eyring | 5040.0 | 0.1872 | 4.4000 |

**Table A5** Regression results for adsorption of $CH_4$, $C_2H_6$ and $C_4H_{10}$, on silicalite (Case E)

| Model | $\alpha_i$ | $\beta_i$ | $\mathrm{Ln}(k_i)$ | *%AAD* |
|---|---|---|---|---|
| | | Methane at 308 K | | |
| SRK | −4464.2 | 0.1963 | −0.3220 | 1.38 |
| PR | −4867.7 | 0.2007 | −0.3143 | 1.33 |
| VDW | −4074.7 | 0.1846 | −0.3340 | 1.47 |
| Eyring | 3924.2 | 0.1365 | 0.0691 | 3.03 |
| | | Methane at 353 K | | |
| SRK | 9525.1 | 0.4402 | −1.4478 | 2.65 |
| PR | 9664.2 | 0.4372 | −1.4353 | 2.65 |
| VDW | 8839.4 | 0.4492 | −1.4478 | 2.47 |
| Eyring | 6379.1 | 0.0824 | −1.2348 | 2.74 |
| | | Methane at 423 K | | |
| SRK | −8561.8 | 0.0835 | −2.6724 | 0.35 |
| PR | −8594.6 | 0.0866 | −2.6724 | 0.35 |
| VDW | −8324.2 | 0.0834 | −2.6740 | 0.33 |
| Eyring | 13741.2 | 0.0987 | −2.5068 | 1.51 |
| | | Ethane at 308 K | | |
| SRK | −160.4 | 0.3380 | 2.6695 | 1.70 |
| PR | −294.5 | 0.3379 | 2.6737 | 1.70 |
| VDW | 1889.5 | 0.3444 | 2.5621 | 1.61 |
| Eyring | 21064.5 | 0.3124 | 3.0636 | 0.78 |
| | | Ethane at 353 K | | |
| SRK | 4827.4 | 0.3487 | 0.9226 | 1.31 |
| PR | 4330.8 | 0.3479 | 0.9913 | 1.20 |
| VDW | 3325.6 | 0.3496 | 0.9490 | 1.05 |
| Eyring | 23551.8 | 0.3103 | 1.4810 | 0.63 |
| | | Ethane at 423 K | | |
| SRK | −16680.9 | 0.0375 | −0.7021 | 2.20 |
| PR | −17294.3 | 0.0448 | −0.6867 | 2.35 |
| VDW | −16283.2 | 0.0309 | −0.7120 | 2.08 |
| Eyring | −14163.4 | 0.0087 | −0.5979 | 2.43 |
| | | *n*-Butane at 308 K | | |
| SRK | −54316.0 | 0.4831 | 10.3463 | 2.64 |
| PR | −59192.0 | 0.4758 | 9.9864 | 2.44 |
| VDW | −61537.8 | 0.3850 | 11.2287 | 4.20 |
| Eyring | −64852.4 | 0.3301 | 14.3542 | 4.92 |
| | | *n*-Butane at 353 K | | |
| SRK | −51823.2 | 0.4832 | 7.5264 | 1.05 |
| PR | −55752.0 | 0.4946 | 7.4866 | 0.96 |
| VDW | −34489.3 | 0.4679 | 7.1927 | 1.08 |
| Eyring | 8439.6 | 0.4461 | 6.9268 | 0.95 |
| | | *n*-Butane at 423 K | | |
| SRK | −30722.1 | 0.3993 | 2.4210 | 0.67 |
| PR | −34469.6 | 0.4090 | 2.4406 | 0.67 |
| VDW | −25970.5 | 0.3489 | 2.3233 | 0.69 |
| Eyring | 25800.4 | 0.4236 | 2.4069 | 1.03 |

## References


Bae, Y.S., Lee, C.H.: Sorption kinetics of eight gases on a carbon molecular sieve at elevated pressure. Carbon **43**, 95–107 (2005)

Calleja, G., Pau, J., Calles, J.A.: Pure and multicomponent adsorption equilibrium of carbon dioxide, ethylene, and propane on ZSM-5 zeolites with different Si/Al ratios. J. Chem. Eng. Data **43**, 994–1003 (1998)

Cochran, T.W., Kabel, R.L., Danner, R.P.: Vacancy solution theory of adsorption using Flory-Huggins activity coefficient equations. AIChE J. **31**, 268–277 (1985)

Craig, R.J.C., Seaton, N.A.: Prediction of multicomponent adsorption equilibrium using a new model of adsorbed phase nonuniformity. Langmuir **13**, 1205–1210 (1997)

Do, D.D.: Adsorption Analysis: Equilibria & Kinetics. Imperial College, London (1998)

Gumma, S.: On measurement, analysis and modeling of mixed gas adsorption equilibria. Ph.D. thesis, Cleveland State University (2003)

Hu, X.: Multicomponent adsorption equilibrium of gases in zeolite: effect of pore size distribution. Chem. Eng. Commun. **174**, 201–214 (1999)

Hu, X., Do, D.D.: Effect of pore size distribution on the prediction of multicomponent adsorption equilibria. In: Levan, M.D. (ed.) Fundamentals of Adsorption, pp. 385–392. Kluwer Academic, Boston (1996)

Hyun, S.H., Daner, R.P.: Equilibrium adsorption of ethane, ethylene, isobutane, carbon dioxide, and their binary mixtures and carbon dioxide on 13X molecular sieves. J. Chem. Eng. Data **27**, 196 (1982)

Mukhopadhyay, M., Raghuram Rao, G.V.: Thermodynamic modeling for supercritical fluid process design. Ind. Eng. Chem. Res. **32**, 922–930 (1993)

Myers, A.L., Prausnitz, J.M.: Thermodynamics of mixed-gas adsorption. AIChE J. **11**, 121–127 (1965)

Novenario, C.R., Caruthers, J.M., Chao, K.C.: A mixing rule to incorporate solution model into equation of state. Ind. Eng. Chem. Res. **35**, 269–277 (1996)

Peng, X., Wang, W., Xue, R., Shen, Z.: Adsorption separation of $CH_4/CO_2$ on mesocarbon microbeads: experiment and modeling. AIChE J. **52**, 994–1003 (2006)

Perry, R.H., Chilton, C.H.: Chemical Engineers' Handbook, 5th edn. McGraw-Hill, New York (1973), pp. 3–246

Pongsiri, N., Viswanath, D.S.: A comparative study of mixing rules in the prediction of solid-vapor equilibria. Ind. Eng. Chem. Res. **28**, 1918–1921 (1989)

Qiao, S., Wang, K., Hu, X.: Study of binary adsorption equilibrium of hydrocarbons in activated carbon using micropore size distribution. Langmuir **16**, 5130–5136 (2000a)

Qiao, S., Wang, K., Hu, X.: Using local IAST with micropore size distribution to predict multicomponent adsorption equilibrium of gases in activated carbon. Langmuir **16**, 1292–1298 (2000b)

Rao, V.S.G., Mukhopadhyay, M.: Covolume-dependent mixing rule for prediction of supercritical fluid-solid equilibria. In: Proceedings of the First International Symposium on Supercritical Fluids, Nice (France), p. 161. Societe Francaise de Chimie, Paris (1988)

Rao, V.S.G., Mukhopadhyay, M.: Effect of covolume dependency of the energy parameter on the predictability of SCFE data using the Peng-Robinson equation of state. J. Supercrit. Fluids **2**, 22 (1989)

Reich, R., Ziegler, W.T., Rogers, K.A.: Adsorption of methane, ethane and ethylene gases and their binary and ternary mixtures and carbon dioxide on activated carbon at 212–301 K and pressure to 35 atmospheres. Ind. Eng. Chem. Process Des. Dev. **12**, 336 (1980)

Ruthven, D.M.: Principles of Adsorption and Adsorption Processes. Wiley, New York (1984)

Semenova, S.I.: Polymer membranes for hydrocarbon separation and removal. J. Membr. Sci. **231**, 189–207 (2004)

Suwanayuen, S., Danner, R.P.: A gas adsorption isotherm equation based on vacancy solution theory. AIChE J. **26**, 68–75 (1980a)

Suwanayuen, S., Danner, R.P.: Vacancy solution theory of adsorption from gas mixtures. AIChE J. **26**, 76–83 (1980b)

Wang, K., Do, D.D.: Characterizing the micropore size distribution of activated carbon using equilibrium data of many adsorbates at various temperatures. Langmuir **13**, 6226–6233 (1997)

Wang, K., Qiao, S., Hu, X.: Application of IAST in the prediction of multicomponent adsorption equilibrium of gases in heterogeneous solids: micropore size distribution versus energy distribution. Ind. Eng. Chem. Res. **39**, 527–532 (2000)

Wojciechowski, B.W., Hsu, C.C., Rudzinski, W.: Adsorption from multicomponent gas mixtures on the heterogenous surfaces of solid catalysts. Can. J. Chem. Eng. **63**, 789–794 (1985)

Wu, Q., Li, Z., Wu, J., Zhou, Y.: Adsorption equilibrium of the mixture $CH_4 + N_2 + H_2$ on activated carbon. J. Chem. Eng. Data **50**, 635–642 (2005)

Yang, R.T.: Gas Separation by Adsorption Processes. Butterworth, Boston (1987)

Zhou, C., Hall, F., Gasem, A.M., Robinson, R.L.: Predicting gas adsorption using two-dimensional equations of state. Ind. Eng. Chem. Res. **33**, 1280–1289 (1994)